RSC Advances

PAPER

View Article Online
View Journal | View Issue

Cite this: *RSC Adv.*, 2020, **10**, 42137

A fluorescent Cu(II) complex as a dual functional sensor for selective and sensitive detection of acetone and Cd(II) pollutants†

Mohd. Muddassir,* Abdullah Alarifi, Mohd Afzal, Khulud Abdullah Alshali, Naaser A. Y. Abduh and Abeer Beagan

In this study, Cu^{2+} perchlorate complexes of 3,5-dimetylpyrazole(dmpy), namely $[Cu(dmpy)_3(H_2O)_2](H_2O)(ClO_4)_2$ (**1**), were prepared and characterized by X-ray diffraction (XRD), thermogravimetric analysis (TGA), infrared (IR) spectroscopy, elemental analysis, mass spectrometry, and ultraviolet visible (UV-Vis) spectroscopy. It was determined that Cu^{2+} coordinated to the nitrogen atoms of three dmpy molecules as well as to the oxygen atoms of two H_2O molecules in a square pyramidal geometry. To balance the charge, two uncoordinated perchlorate anions and one H_2O molecule were also present in the lattice. The resulting Cu^{2+} complex was involved in extensive hydrogen bonding, which stabilized the structure. The fluorescence properties of complex **1** were studied in acetonitrile at room temperature upon the addition of different organic solvents. It was confirmed that the complex exhibited remarkable acetone selectivity *via* a fluorescence quenching mechanism. At low concentrations, the fluorescence intensities were nearly completely quenched *via* a turn-off mode. Moreover, complex **1** displayed exceptional selectivity, fast detection time, and high sensitivity for Cd^{2+} in aqueous solutions *via* a fluorescence enhancement mechanism (turn-on mode). Hence, the prepared complex showed potential for application in Cd^{2+} detection. Notably, in an aqueous solution, complex **1** exhibited highly selective fluorescence enhancement effects (turn-on mode) with respect to Cd^{2+} and was not affected by the interference of other metal ions.

Received 21st September 2020
Accepted 2nd November 2020

DOI: 10.1039/d0ra08073j

rsc.li/rsc-advances

1. Introduction

Acetone is a toxic chemical widely found in the environment. Due to its volatility, acetone poisoning can occur through different pathways, including inhalation, ingestion, or direct skin contact. It can affect cardiovascular and digestive systems; however, it is most harmful to the central nervous system. Acetone also causes toxicity to the respiratory tract and urinary system.[1] It has been determined that acetone remains in the environment, in which it is released. For instance, it was shown that upon its release into water, >99% of acetone persisted in the same environment. The absorbed chemical is distributed throughout the body, particularly affecting organs with high water content, which leads to metabolic disorders and severe damage to various systems.[2–4]

Furthermore, Cd^{2+} is a toxic heavy metal associated with different adverse effects as well as occupational and environmental concerns.[5] Healthy levels of Cd^{2+} in the blood are <5.0 ng mL^{-1}, with most results in the range of 0.5–2.0 ng mL^{-1}. Acute toxicity is observed when the level of Cd^{2+} in the blood exceeds 50 ng mL^{-1}, which leads to high blood pressure, anemia, pulmonary fibrosis, prostrate cancer, lung cancer, yellow discoloration of the front teeth near the gum line, and anosmia.[6–9] The World Health Organization (WHO) reported that the tolerable weekly intake of Cd^{2+} is in the range of 0.007–0.5 mg kg^{-1} of body weight.[10] Most of Cd^{2+} in wastewater originates from oil refining, solid waste incineration, coal and gold mining, fossil fuel combustion, rubber processing, and fertilizer industries. Its presence in water is a major environmental and health problem. Hence, the design and synthesis of new sensors for the efficient, selective, and sensitive detection of acetone and Cd^{2+} is essential in the fields of chemistry, environmental science, and biology.

Supramolecular coordination complexes are discrete constructs typically obtained by mixing soluble metal and ligand precursors, which spontaneously form metal–ligand bonds, generating a single thermodynamically favored product. Several ligands, such as nitrogen, oxygen, and sulphur-based ones, can stabilize metal complexes. Moreover, due to the electron donating ability of their nitrogen atoms, pyrazole-based ligands have been recently extensively studied. Pyrazole

Catalytic Chemistry Research Chair, Department of Chemistry, College of Science, King Saud University, Riyadh 11451, Saudi Arabia. E-mail: mmohammadarshad@ksu.edu.sa; muddassirchem@gmail.com

† Electronic supplementary information (ESI) available. CCDC 1905852. For ESI and crystallographic data in CIF or other electronic format see DOI: 10.1039/d0ra08073j

derivatives have been applied in many fields, including the biological and pharmaceutical industries. Based on the photophysical properties of these compounds, they have also been utilized in gas storage, luminescence, catalysis, magnetic materials, and most importantly for the purposes of this study, chemical sensing.[11–18] Fluorescence sensing based on luminescent coordination complexes has attracted significant attention. It is characterized by a short response time, low cost, as well as high sensitivity and efficiency. In recent years, different coordination-based fluorescent sensors have been established.[19–22] They have been employed to probe small organic molecules and metal ions *via* fluorescence enhancing or quenching. Nevertheless, the rational design and synthesis of luminescent coordination complexes with exhibiting the desired structure and properties remain challenging. Consideration of factors, such as the reaction time, pH, as well as choice of the auxiliary ligand and metal center, which affect the framework structure and properties of the resulting coordination complexes, is essential.[23] Due to their biological significance and structure–activity relationship, numerous studies on the biological and luminescence properties of Cu ions have been conducted. In addition, owing to its presence in many metalloproteins, Cu is ubiquitous in various biological systems. Cu^{2+}-based pyrazole as well as its derivative complexes have been studied for several years because of their remarkable properties both in the solid state[15,24–26] and in solution.[27,28] The pioneering work by Yang and coworkers demonstrated the great potential of a Cu complex, namely $[Cu(tpp)\cdot H_2O]_{2n}$ [Htpp = 1-(4-tetrazol-5″-yl)benzyl-3-(pyraziny-l)pyrazole], in the detection of acetone and Fe^{3+} ions through fluorescence quenching. The developed complex exhibited high sensitivity and selectivity.[29] Moreover, Tripathi's group recently reported a copper terephthalate-based molecular organic framework (MOF). In this case, terephthalic acid was extracted from small pieces of waste soft-drink bottles *via* alkaline hydrolysis. The complex could be used as a sensor for acetone (detection limit of ~20 ppm) with high sensitivity and selectivity.[30]

Nonetheless, the majority of examples involve fluorescence quenching using coordination complexes, while fluorescence enhancement (turn-on) or fluorescence shift is reported less frequently. Compared with the other two methods of fluorescence detection, "turn-on" exhibits higher sensitivity and is simpler. Thus, the development of new luminescent materials, which could be used as turn-on-based chemical sensors, is crucial. To continue our research on luminescent coordination materials, in the present study, we focused on the design and synthesis of a Cu^{2+}-based dual-functional fluorescent sensor for the detection of acetone *via* fluorescent quenching (turn-off). Additionally, the sensor could be used for the detection of Cd^{2+} ions *via* a fluorescence enhancement (turn-on) mode. We report a dmpy-based Cu^{2+} complex, namely $[Cu(dmpy)_3(H_2O)_2](H_2O)(ClO_4)_2$ (**1**), in which the dmpy group is coordinated to the Cu^{2+} ion in a monodentate fashion through its nitrogen atom. The perchlorate anion acts as a counter ion and participates in specific electrostatic or hydrogen bonding interactions with the neighboring H_2O molecules. Furthermore, we determined the molecular structure of **1** with a pentacoordinated Cu center in the crystalline phase by single crystal X-ray diffraction (XRD) analysis. The structural evaluation was complemented by Fourier transform infrared (FTIR) spectroscopy and ultraviolet visible (UV-Vis) spectroscopy, while the thermal stability of the complex was investigated by thermogravimetric analysis (TGA).

2. Experimental

2.1. Materials

All reagents were of the highest commercial grade and were used without further purification.

2.2. Methods and apparatus

Microanalysis (CHN) was performed employing Carlo Erba Analyzer Model 1108, Interspec 2020. Molar conductivity was measured at room temperature using Digsun electrical conductivity meter. An FTIR spectrometer was used for recording the IR spectra of KBr pellets in the range of 4000 to 400 cm^{-1}. The electronic spectra were recorded on a UV-1700 PharmaSpec UV-Vis spectrophotometer (Shimadzu). The emission spectra were acquired on a Shimadzu RF-6000 fluorescence spectrophotometer. A pass width of 10 nm was used for the measurement of the emission and excitation spectra. All measurements were performed under identical experimental conditions. TGA and differential scanning calorimetry (DSC) were performed using a Universal V3.8 B TA SDT Q600 Build 51 thermal analyzer under a nitrogen atmosphere using alumina powder as a reference material.

2.3. Synthesis

The complex was obtained by dissolving dmpy (3 mmol, 0.228 g) and $CuClO_4\cdot 6H_2O$ (1 mmol, 0.371 g) in 20 mL of MeOH and stirring the solution at room temperature for 2 h. The resulting clear blue solution was slowly evaporated. After four days, the formed needle-shaped blue crystals were washed with hexane and stored for further analysis. Yield 73%; elemental analysis for $C_{15}H_{30}Cl_2CuN_6O_{11}$: C 29.78%, H 5.00%, N 13.89%; found: C 30.40%, H 4.96%, N 13.98%.

X-ray crystal structure determination, topological analysis, and details of the fluorescence titrations are described in the supplementary material† (CCDC number: 1905852).

3. Results and discussion

3.1. Product characterization

The synthesized product was characterized by XRD, TGA, FTIR spectroscopy, elemental analysis, mass spectrometry, and UV-Vis spectroscopy. All analyses supported the structure of the product shown in Scheme 1. Importantly, complex **1** was stable to air and moisture.

3.2. X-ray structure of $[Cu(dmpy)_3(H_2O)_2](H_2O)(ClO_4)_2$ (1)

The ball-stick model of $[Cu(dmpy)_3(H_2O)_2](H_2O)(ClO_4)_2$ is shown in Fig. 1. As it can be seen, the complex crystallized in the triclinic space group $P\bar{1}$ ($Z = 2$) with a pentacoordinated copper

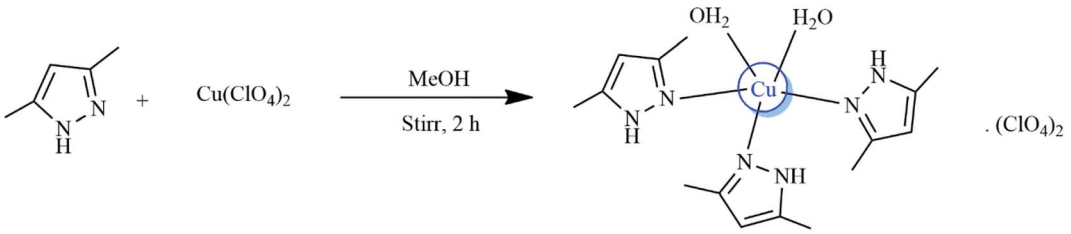

Scheme 1 Synthesis of $[Cu(dmpy)_3(H_2O)_2](H_2O)(ClO_4)_2$ (**1**).

center. The important parameters of complex **1** are summarized in Table 1.

As shown in Fig. 1(a), the Cu^{2+} anion coordinated to the nitrogen atoms of the three dmpy molecules as well as to the oxygen atoms of two H_2O molecules. The coordination polyhedron of the Cu^{2+} atom was tetragonal pyramidal (CN = 5). To achieve charge balance, two uncoordinated perchlorate anions and one H_2O molecule are also present in the lattice and are involved in extensive hydrogen bonding (Fig. 1(b)).

The Cu–N bond distances were in the range of 1.987(2)–1.991(2) Å, whereas the Cu–O bond distances were in the range of 1.9784(19)–2.2278(18) Å. These values were consistent with those previously reported for similar Cu^{2+} complexes (Table 2).[27,28] Surprisingly, there was a difference in the bond lengths of the coordinated H_2O molecules, which was attributed to hydrogen bonding. All bond angles were in the range of 86.83(8)–170.70(8)°. Notably, all bond lengths and angles were in agreement with those previously established for similar complexes.[23,24,31,32] The prepared molecule exhibited extensive hydrogen bonding between the bonded and lattice H_2O molecules, bonded dmpy molecules, and non-bonded perchlorate anions. Specifically, two of the dmpy molecules displayed hydrogen bonding to two perchlorate anions, while the third dmpy (N1) molecule was not involved in any hydrogen bonding interactions. The oxygen atoms of both perchlorates (*i.e.*, O5 and O8) showed intermolecular N–H···O interactions with the hydrogen atoms of the bonded dmpy molecule (2.897(3)–2.967(3) Å). Both of the coordinated H_2O molecules (*i.e.*, O1 and O2) exhibited hydrogen bonding interactions with the lattice H_2O molecule (*i.e.*, O3) as well as with two perchlorate anions (*i.e.*, O5, O9, and O8) in the range of 2.725(3)–3.019(3).

The second coordinated H_2O molecule showed weak hydrogen bonding interactions with the neighboring perchlorate anions. As a result, the perchlorate anions weakly coordinated to Cu^{2+} (2.2278 (18) Å). The two perchlorate anions and the lattice H_2O molecule exhibit strong intramolecular adhesive

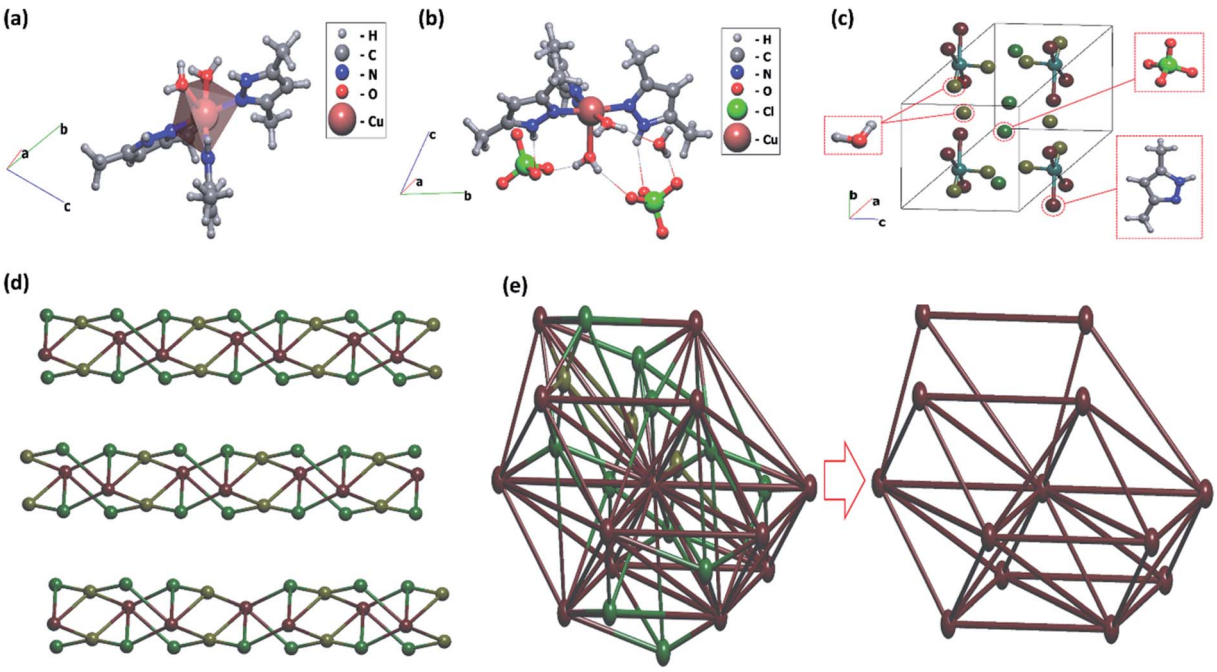

Fig. 1 (a) Coordination polyhedron of the Cu^{2+} atom (ball-stick model) in complex **1**. (b) Hydrogen bonding interactions in complex **1**. (c) The underlying net in the standard representation. Cyan spheres correspond to the copper atoms, brown spheres indicate the dmpy ligands, olive spheres refer to H_2O molecules, and green spheres correspond to the ClO_4^- anions. (d) The underlying net in the standard representation of the hydrogen-bonded molecular structure. Brown spheres correspond to the $C_{15}H_{28}N_6O_2Cu$ complex, olive spheres refer to H_2O, while green spheres indicate ClO_4^-. (e) Molecular packing of all SBUs (left) and the $C_{15}H_{28}N_6O_2Cu$ complex (right).

Table 1 Crystal data and structure refinement for $[Cu(dmpy)_3(H_2O)_2](H_2O)(ClO_4)_2$ (1)

CCDC No	CCDC 1905852
Chemical formula	$C_{15}H_{28}CuN_6O_2 \cdot 2(ClO_4) \cdot H_2O$
M_r	604.89
Crystal system, space group	Triclinic, $P\bar{1}$
Temperature (K)	150
a, b, c (Å)	10.1667 (12), 12.3453 (13), 12.6574 (15)
α, β, γ (°)	62.592 (4), 68.790 (5), 68.138 (4)
V (Å^3)	1273.5 (3)
Z	2
Radiation type	Mo Kα
μ (mm^{-1})	1.13
Crystal size (mm)	0.05 × 0.05 × 0.04
Data collection	
Diffractometer	Bruker AXS D8 quest CMOS diffractometer
Absorption correction	Multi-scan SADABS 2016/2: L. Krause, R. Herbst-Irmer, G. M. Sheldrick & D. Stalke, *J. Appl. Crystallogr.* **48** (2015) 3–10
T_{min}, T_{max}	0.710, 0.746
No. of measured, independent, and observed [$I > 2s(I)$] reflections	76 237, 7831, 5408
R_{int}	0.096
(sin $\theta/\lambda)_{max}$ (Å^{-1})	0.717
Refinement	
$R[F^2 > 2s(F^2)]$, w$R(F^2)$, S	0.050, 0.104, 1.05
No. of reflections	7831
No. of parameters	340
No. of restraints	6
H-atom treatment	H atoms treated by a mixture of independent and constrained refinement
$\Delta\rho_{max}$, $\Delta\rho_{min}$ (e Å^{-3})	0.80, −0.50

Table 2 Selected bond lengths (Å) and bond angles (°) of $[Cu(dmpy)_3(H_2O)_2](H_2O)(ClO_4)_2$ (1)

N1–Cu1	1.987 (2)	N3–Cu1	1.991 (2)
N5–Cu1	1.990 (2)	O2–Cu1	2.2278 (18)
O1–Cu1	1.9784 (19)		
C2–N1–Cu1	128.35 (17)	N2–N1–Cu1	125.62 (16)
C7–N3–Cu1	131.08 (17)	N4–N3–Cu1	123.53 (15)
C12–N5–Cu1	134.20 (18)	N6–N5–Cu1	120.18 (15)
Cu1–O1–H1D	120 (2)	Cu1–O1–H1E	121 (2)
Cu1–O2–H2A	125 (2)	Cu1–O2–H2B	115 (2)
O1–Cu1–N1	86.83 (8)	O1–Cu1–N5	88.65 (8)
N1–Cu1–N5	170.70 (8)	O1–Cu1–N3	169.34 (9)
N1–Cu1–N3	91.93 (8)	N5–Cu1–N3	91.01 (8)
O1–Cu1–O2	92.95 (8)	N1–Cu1–O2	91.30 (8)
N5–Cu1–O2	97.05 (8)	N3–Cu1–O2	97.66 (8)

forces and several of the oxygen atoms are involved in hydrogen bonding. Hence, the inter- and intramolecular hydrogen bonding in the complex is extensive. All copper atoms, centers of mass of the organic ligands, perchlorate anions, and water molecules are nodes of the underlying net in the standard representation of the valence-bonded structures. The underlying 1,5-c net of the 1,5M6-1 topological type is shown in Fig. 1(c).

The standard description of a hydrogen-bonded crystal typically involves a simplification procedure, *i.e.*, representation of the molecular network in terms of a graph theory approach, taking into account hydrogen bonds between molecules. The simplification procedure usually consists of representing the molecule by its center of mass, retaining the connectivity of the molecule with its neighbors. All intermolecular contacts between a given pair of molecules are transformed to the same edge between the molecular centers of mass in the simplified net. Hence, such a description characterizes the way the molecules are hydrogen-bonded in the crystal. In this work, the standard representation of the structure resulted in the 1D underlying net of a new topological type (Fig. 1(d)). Furthermore, a description of the molecular packing can be obtained by taking into account all intermolecular contacts during the simplification procedure. The conducted calculations revealed that the 3D underlying 5,9,9,27-c net of such a package corresponded to a new topology with a point symbol for the following net: $\{3^{18}\cdot4^{18}\}\{3^{19}\cdot4^{17}\}\{3^{8}\cdot4^{2}\}\{3^{81}\cdot4^{176}\cdot5^{90}\cdot6^{4}\}$ (Fig. 1(e), left). The package predominantly included large complexes; therefore, molecules of H_2O and ClO_4^- anions were removed prior to simplification. The obtained 3D underlying 12-c net was of a "bcu-x/14-conn; $Im\bar{3}m > P2_1/c$ $(1/2a + 1/2b + 1/2c, 2a - 2b, -c; 1/2, 0, 1/2)$; bond sets: 1,2,4,5,7,8,9:bcu-x" topological type (Fig. 1(e), right).

Hence, the intramolecular hydrogen bonding evidently stabilized the molecule. All data, expressed as D···A contacts, are summarized in Table 3.

3.3. Thermogravimetric studies

TGA of complex **1** was conducted to investigate the pyrolysis pattern in temperature range of 25–800 °C. The thermogram of the complex shown in Fig. 2(a) exhibits weight loss in four steps over temperature ranges of 50–255 °C, 260–370 °C, 372–600 °C, and 610–800 °C. Importantly, these results were in good

Table 3 Hydrogen bond geometry (Å, °) of $[Cu(dmpy)_3(H_2O)_2](H_2O)(ClO_4)_2$ (**1**)[a]

D–H···A	D–H	H···A	D···A	D–H···A
N2–H2···O2	0.88	2.56	3.050 (3)	115.7
N2–H2···O5	0.88	2.47	3.141 (3)	133.0
N2–H2···O8i	0.88	2.34	3.071 (3)	140.5
N4–H4···O5	0.88	2.02	2.897 (3)	171.0
N6–H6···O8	0.88	2.13	2.967 (3)	159.7
O1–H1D···O3	0.844 (18)	1.896 (19)	2.731 (3)	170 (3)
O1–H1E···O3ii	0.837 (18)	1.902 (19)	2.725 (3)	167 (3)
O2–H2A···O8	0.798 (18)	2.14 (2)	2.912 (3)	163 (3)
O2–H2B···O5i	0.809 (17)	2.53 (3)	2.961 (3)	115 (3)
O2–H2B···O9i	0.809 (17)	2.24 (2)	3.019 (3)	161 (3)
O3–H3A···O4iii	0.823 (18)	2.03 (2)	2.793 (3)	154 (3)
O3–H3B···O10i	0.831 (18)	2.07 (2)	2.882 (3)	165 (3)

[a] Symmetry codes: (i) $-x+1, -y, -z+1$; (ii) $-x, -y, -z+1$; (iii) $x-1, y, z$.

agreement with the proposed structure. The three H_2O molecules in the system (*i.e.*, two coordinated and one lattice H_2O) were removed in a single step (~9% weight loss) in the temperature range of 50–255 °C. In addition, the noticeable weight loss of nearly 48% at 260–370 °C indicated the removal of the 3,5-dimethylpyrazole group. The decomposition of the perchlorate ions, which was evidenced by a 33% weight loss, occurred in the temperature range of 372–600 °C. Finally, the TGA curve showed a plateau at temperatures above 610–800 °C, which corresponded to the formation of Cu oxide species as the final products.

3.4. FTIR spectroscopy

The FTIR spectrum of complex **1** is illustrated in Fig. 2(b). As it can be seen, the spectrum exhibits an absorption band at 3155 cm^{-1} corresponding to the N–H bond originating from the monodentate coordination of 3,5-dimethylpyrazole. The absorptions attributed to the 3,5-dimethylpyrazole ligand observed between 1650–1250 cm^{-1} were consistent with the coordination of the nitrogen atom to the Cu^{2+} center.[31] Furthermore, a ν(OH) band was detected at 3511 cm^{-1} and was attributed to the presence of coordinated H_2O molecules. In contrast, the peak at ~3338 cm^{-1} corresponded to the lattice H_2O molecule. The coordination of the H_2O molecules to the Cu^{2+} ions was further confirmed by the appearance of the non-ligand band at 812 cm^{-1}, which was ascribed to the rocking mode of H_2O.[33] The spectrum of the free dmpy ligand showed peaks at 1028, 1010, and 404 cm^{-1}. The same absorption bands were also observed as sharp signals in the spectrum of complex **1**; however, they shifted to a higher frequency, confirming the coordination of the ligand to Cu^{2+}.[31] The crystal structure analysis of the Cu^{2+} complex **1** demonstrated the lack of interactions between the metal centers and the anion. Nevertheless, as stated above, there were several hydrogen bonding interactions between dmpy, coordinated/lattice water molecules, and perchlorate oxygen atoms. The T_2 mode at ~1100 cm^{-1} was detected as an intense band, which is characteristic of perchlorate anions. Several smaller bands were observed in the region between 600 and 750 cm^{-1}, which indicated the presence of significant interactions between the perchlorate group and the cation in the complex.[34]

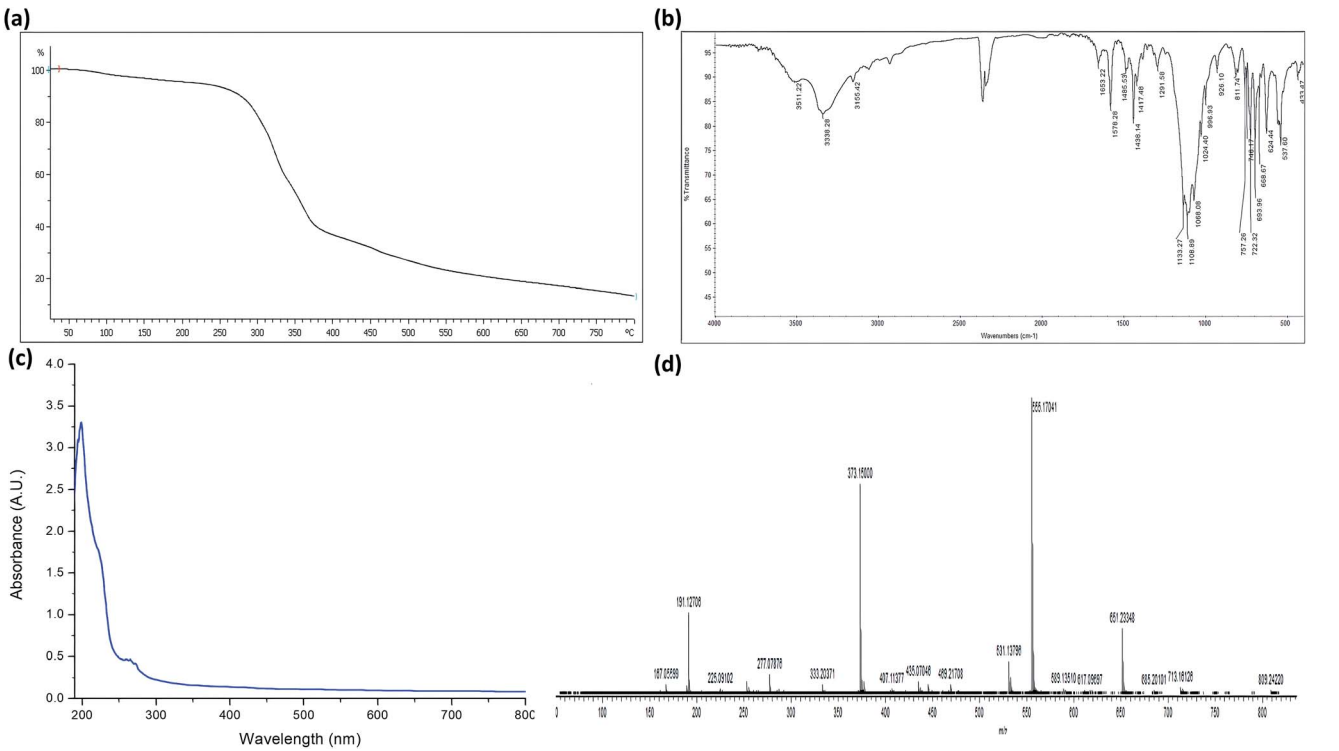

Fig. 2 (a) TGA of complex **1**. (b) FTIR spectrum of complex **1**. (c) Absorption spectrum of complex **1**. (d) Mass spectrum of complex **1**.

The splitting observed in this region of the spectrum was attributed to various factors. It is known that the fingerprint region is generally less informative than the lower energy part of the spectrum. The formation of the Cu^{2+} complex was further confirmed by the existence of medium intensity bands in the region of 413–415 cm^{-1}, which were assigned to ν(Cu–O) and ν(Cu–N).[35]

3.5. Electronic spectrum

The electronic spectrum of complex **1** shown in Fig. 2(c) displayed intense absorption bands at 199 nm, which corresponded to the n → π* transition. Moreover, complex **1** exhibited an intense transition at 267 nm, which was attributed to the intra-ligand π → π* transition. A low energy broadband was detected in the visible region at 516 nm and was ascribed to the Cu^{2+} d → d transition. This result was consistent with the distorted square planar environment around the Cu^{2+} ion.

3.6. Solid-state photoluminescence spectra

We subsequently obtained photoluminescence spectra of complex **1** and free dmpy. Upon excitation at 267 nm, complex **1** exhibited a small emission band at 492 nm and a strong emission band at 619 nm (ESI, Fig. S3†). In contrast, the spectrum of dmpy showed a broad band at 360 nm, which was assigned to the internal π → π* transitions (ESI, Fig. S2(b)†). Moreover, in the spectrum of **1**, the intense emission band at 492 and 619 nm was attributed to the ligand-to-metal charge transfer.

3.7. Mass spectrometry

The complex was unambiguously characterized by mass spectrometry analysis. The electrospray mass spectra of **1** showed the molecular ion peak as well as signals resulting from the fragmentation of the complex (Fig. 2(d)). The molecular ion peak at *m*/*z* 555 corresponded to $\{[Cu(dmpy)_3(H_2O)_2](H_2O)(ClO_4)_2–3H_2O + 4H^+\}v$ formed by the removal of labile H_2O molecules.

3.8. Fluorescence sensing properties

The previously reported sensors were predominantly focused on lanthanide-based complexes. Despite the fact that d^{10} metal ion-based coordination complexes (*e.g.*, Zn^{2+}, Cd^{2+}, and Hg^{2+}) have shown remarkable acetone sensing properties, only a few sensors based on these structures have been reported. Unlike in the case of lanthanide-based complexes, structures based on d^{10} metals do not require preheating, pH change, or removal of the solvent from the system, which could hinder the solvent molecules from interacting with metal ions.[36–41] Moreover, the potential of Cu^{2+}-based complexes as fluorescence sensors has also been demonstrated.[42] For example, Amilan Jose *et al.* reported the detection of water in various organic solvents, such as methanol, tetrahydrofuran (THF), acetonitrile, and acetone, using fluorescence emission intensity in the presence of a Cu complex probe.[43]

The luminescence properties of complex **1** dissolved in acetonitrile were studied at room temperature. It was found that **1** exhibited an intense emission band at λ_{em} = 650 nm (λ_{ex} = 267 nm). The formation of supramolecular interactions can sometimes increase the rigidity of a molecule and enhance the intra- or intermolecular interactions between ligands, which can be favorable for energy transfer.[41] The fluorescence sensing experiments were performed by dissolving complex **1** in acetonitrile and subsequently adding other organic solvents, such as chloroform, toluene, ethylbenzene, carbon tetrachloride (CCl_4), benzene, dichloromethane (DCM), dimethylsulfoxide (DMSO), dimethylformamide (DMF), benzyl alcohol, *iso*-butanol, methanol, *iso*-propanol, ethanol, and acetone. As illustrated in Fig. 3(a), only the addition of acetone effectively quenched the fluorescence emissions of **1**. Almost complete quenching (*i.e.*, a 95% decrease in the emission intensities of **1**) was observed upon the addition of acetone. In contrast, no decrease in the emission intensities was observed after addition of similar volumes of other solvents. While some quenching of the emission intensity of complex **1** was noted following the addition of alcoholic solvents, acetone exhibited the most evident effects.

It was also found that the quenching efficiency of acetone with respect to complex **1** was not affected by the existence of other organic molecules, demonstrating high selectivity (Fig. 3(b)).

The results revealed that complex **1** could selectively sense the acetone molecules and exhibited a relatively low acetone detection limit compared with other previously reported transition metal-based sensors. Importantly, unlike in the case of lanthanide-based complexes, **1** could be used for acetone sensing without activation.[37,38] To examine the sensitivity of complex **1** for sensing acetone in more detail, the quenching efficiencies of **1** dissolved in acetonitrile were investigated at increasing amounts of acetone. As shown in Fig. 3(c), the fluorescent quenching efficiency rapidly increased at low concentrations of acetone. When the acetone concentration increased from 5.0×10^{-6} to 8.0×10^{-5} M, the fluorescence intensity was quenched by nearly 95%. The value of the association constant was determined to establish the strength of the binding between complex **1** and acetone at an increasing concentration of the solvent. The quantitative analysis was conducted using the Stern–Volmer (S–V) equation. The S–V plots exhibited straight lines at different acetone concentrations, demonstrating good linearity at low concentrations (ESI, Fig S1(a)†). In addition, the binding constant was calculated at 1.02×10^3 M^{-1} (R^2 =0.9973), which is significantly greater than the values for previously reported fluorescent acetone sensors.[44]

The high value of the association constant demonstrated the remarkable potential of **1** for the detection of trace amounts of acetone. Furthermore, as shown in Fig. S1(b),† the corresponding detection limit obtained from the 3δ/slope 42 (δ: standard error) reached 1.78×10^{-5} M (R^2 = 0.9856), which was lower than those of previously reported acetone sensors.[45]

To determine whether the fluorescence quenching occurred by complex **1** and not by dmpy, we conducted a control experiment involving addition of increasing amounts of acetone to a homogeneous solution of the dmpy in acetonitrile. As

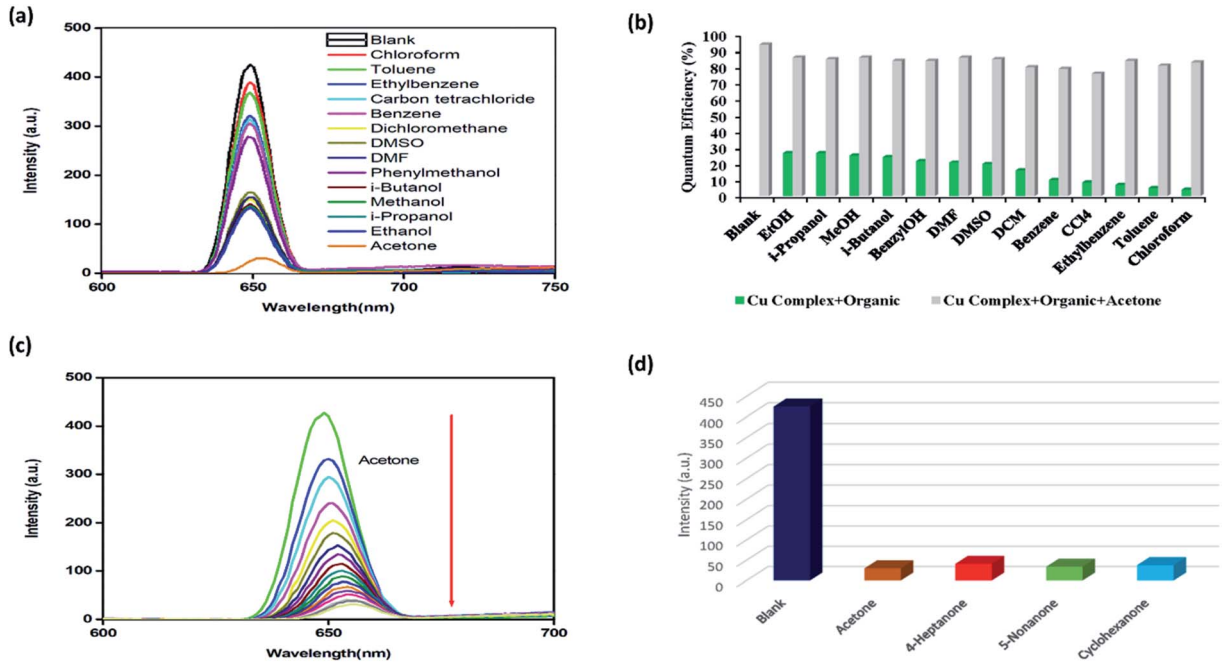

Fig. 3 (a) Fluorescence spectra of complex **1** dissolved in acetonitrile (blank) and upon the addition of different organic solvents. (b) Quenching efficiency of complex **1** upon the addition of different organic solvents except for acetone (green), and following the subsequent addition of acetone (grey). (c) Change in the fluorescence intensity of **1** dissolved in acetonitrile (blank) upon titration with acetone. (d) Fluorescence intensity of complex **1** in various ketone solvents.

demonstrated in Fig. S2(b),† the successive addition of acetone did not cause any fluorescence quenching, indicating that quenching was specific to the structure of complex **1**.

Furthermore, the low detection limit suggested that complex **1** exhibited highly sensitive acetone sensing abilities. Hence, **1** is proposed as a potential candidate for the selective sensing of acetone. The results of our study are consistent with the outcomes of previous works on acetone sensing, *e.g.*, those reported by Zhang and coworkers.[46] In addition, it was speculated that the mechanism of the fluorescent quenching of **1** during the detection of acetone could involve an inner filter effect (IFE) between **1** and the acetone molecules.[47,48] It is noteworthy that the absorption spectrum of acetone (~270 nm) overlapped with the excitation peak of complex **1** (267 nm).[49] Upon excitation, competition for absorption of the light source energy occurred between the acetone molecules and **1**. Thus, the large overlap between the absorption spectrum of acetone and the excitation spectrum of **1** is a consequence of this competition, which also lead to IFE and fluorescent quenching.[46]

Moreover, the C=O moiety of acetone could form hydrogen bonding interactions with dmpy. An electron transfer from dmpy to acetone during excitation might lead to luminescence quenching. Additionally, the selective fluorescence quenching effect observed in the presence of acetone could be attributed to the lone pair$\cdots\pi$ interactions between the dmpy moiety of complex **1** and the C=O group of acetone, which formed a stable acetone–Cu^{2+} adduct.

To establish whether the interactions between the C=O moiety of acetone and the framework of complex **1** resulted in fluorescence quenching, we evaluated the fluorescence behavior of **1** immersed in different ketone solvents. As shown in Fig. 3(d), the solutions of **1** in cyclohexanone, 4-heptanone, and 5-nonanone exhibited the strongest quenching. These results suggested that the fluorescence quenching might be caused by the interactions between the C=O groups and the framework of **1**. Thus, it was determined that complex **1** as well as other Cu-based complexes could be considered as potential candidates for selective sensing of different ketone molecules. It is widely known that the physical interactions between the solute and solvent play a vital role in the fluorescence enhancing and quenching effects of small solvent molecules. Although sensing of acetone by **1** was not superior to using d^{10} metal or lanthanide-based systems, the complex developed herein shows better sensing capabilities than other transition metal-based coordination complexes. Cu-based complexes are typically utilized for the detection of water or anions in different solvents; therefore, application of **1** for the detection of acetone is a new finding.

3.9. Sensing of metal ions

The existence of Lewis basic nitrogen active sites in the structure of **1** means that the complex could be a promising candidate for sensing and detecting metal ions. In this work, to assess the capability of **1** to detect metal ion species, the complex was immersed in an aqueous solution of MCl_x (M = Ba^{2+}, Co^{2+}, Cr^{3+}, Mn^{2+}, Cu^{2+}, Hg^{2+}, K^{+}, Li^{+}, Mg^{2+}, Na^{+}, Ni^{2+}, Pb^{2+}, Al^{3+}, Zn^{2+}, Cd^{2+}, and Ag^{+}). The luminescence spectra of the solutions were recorded analyzed. As shown in Fig. 4(a), the obtained fluorescent spectra demonstrated that for most of the studied metal

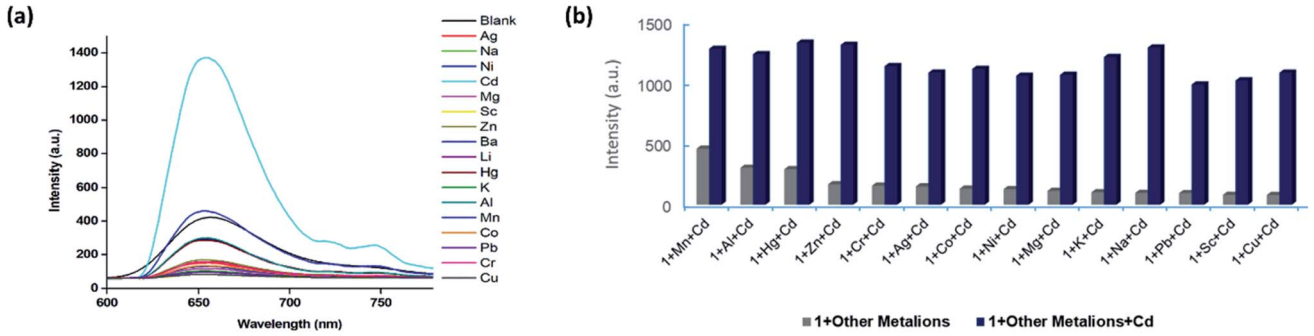

Fig. 4 (a) Fluorescence spectra of complex **1** dissolved in acetonitrile (blank) and upon the addition of aqueous solutions of different metal ions. (b) Fluorescence intensities of **1** in the presence of aqueous solutions of various metal ions with (blue) and without Cd^{2+} ions (grey).

ions, the fluorescence intensity did not change significantly, with the exception of Cd^{2+} (turn-on effect).

The high selectivity for Cd^{2+} was attributed to the suitable coordination geometry and conformation of the nitrogen heterocycle. We also conducted X-ray photoelectron spectroscopy (XPS) analysis of Cd^{2+}/**1** after the fluorescence measurements. The XPS spectrum exhibited a typical peak corresponding to Cd^{2+} at 405.4 eV as well as a peak attributed to Cu^{2+} at 933 eV. These results confirmed the existence of Cd^{2+} ions in the framework of complex **1** (Fig. S4†). Based on the above outcomes, it was speculated that Cd^{2+} ions might interact with the dmpy ligand through Lewis acid–base interactions, promoting a more efficient energy transfer from the ligand to the Cu^{2+} ions. This resulted in turn-on luminescence behaviour of **1** and high selectivity and sensitivity toward Cd^{2+} ions.

Precise detection of specific metal ions in mixed solvent systems is crucial. Thus, we subsequently investigated the selectivity of the prepared complex in the presence of interferences. An aqueous solution of Cd^{2+} was added into aqueous solutions containing complex **1** and various metal ions, and the changes of the fluorescence intensity were monitored. As shown in Fig. 4(b), clear differences between the emission of Cd^{2+} and other cations were observed, which indicated that **1** was a promising luminescent probe for the detection of Cd^{2+} ions. Notably, the experiments showed that the fluorescence detection of **1** was not interfered by the presence of other metal ions, further demonstrating the remarkable selectivity of the complex.

It was determined that complex **1** displayed strong fluorescence, which was measurable even at lower concentrations. It exhibited fluorescence quenching (turn-off) and fluorescence enhancement (turn-on) in the presence of acetone and Cd^{2+} ions in aqueous environments. Hence, the present study demonstrated that fine-tuning of the structural features in **1** could lead to the development of new efficient materials for various applications.

4. Conclusions

In this study, Cu^{2+} perchlorate complexes of 3,5-dimethylpyrazole, namely $[Cu(dmpy)_3(H_2O)_2](H_2O)$ $(ClO_4)_2$ (**1**), were prepared and characterized by XRD, TGA, FTIR, elemental analysis, mass spectrometry, and UV-Vis spectroscopy. The presence of extensive intermolecular hydrogen bonding interactions in the complex stabilized the structure. The presence of intermolecular interactions in the complex enabled its application in fluorescence sensing. Importantly, the prepared complex **1** was determined to be stable towards air and moisture. It exhibited highly sensitive and selective fluorescence quenching (turn-off) effect in the presence of acetone as well as fluorescence enhancement (turn-on) effect toward Cd^{2+} ions in aqueous solutions. In addition, the plausible mechanism for fluorescence quenching of acetone was elucidated. We concluded that the fluorescence quenching was attributed to the interactions between the C=O bond of acetone and the framework of **1** as well as the interactions between the Cu^{2+} ion and acetone. We speculated that the mechanism of fluorescence enhancement of Cd^{2+} ions might involve Lewis acid–base interactions of the metal ions with the dmpy ligand, which promoted a more efficient energy transfer from the ligand to the Cu^{2+} ions, resulting in turn-on luminescence behaviour of **1**. It was established that the complex showed high selectivity and sensitivity toward Cd^{2+} ions. This article describes a promising approach for the design of multi-functional Cu^{2+}-based sensors for both acetone and Cd^{2+} ions. The results described herein will be useful for further experiments conducted under more realistic conditions, which would expand the scope of utilization of Cu^{2+}-containing complexes (*e.g.*, DNA binding, DNA cleavage, cancer studies, and catalysis). Further studies will provide new insights into the nature of this important class of metal complexes and enable the design novel multifunctional metallosystems for applications in material science and diagnosis.

Conflicts of interest

There are no conflicts to declare.

Acknowledgements

The authors extend their sincere appreciation to the Deputyship for Research & Innovation, "Ministry of Education" in Saudi Arabia for funding this research work through the project number IFKSURG–1440–076.

References

1 D. Han and M. Zhao, Facile and simple synthesis of novel iron oxide foam and used as acetone gas sensor with sub-ppm level, *J. Alloys Compd.*, 2020, **815**, 152406.
2 A. A. Baharuddin, B. C. Ang, A. S. M. A. Haseeb, Y. C. Wong and Y. H. Wong, Advances in chemiresistive sensors for acetone gas detection, *Mater. Sci. Semicond. Process.*, 2019, **103**, 104616.
3 M. Muddassir, M. Usman, A. Alarifi, M. Afzal, K. Abdullah Alshali, A. Beagan, A. Kumar, N. A. Y. Abduhd and M. Ahmad, Experimental Sensing and DFT Mechanism of Zn(II) Complex for Highly Sensitive and Selective Detection of Acetone, *Crystals*, 2020, **10**, 324.
4 Y. L. Li, Y. Zhao, P. Wang, Y. S. Kang, Q. Liu, X. D. Zhang and W. Y. Sun, Multifunctional metal-organic frameworks with fluorescent sensing and selective adsorption properties, *Inorg. Chem.*, 2016, **55**, 11821–11830.
5 B. Bali Prasad, D. Jauhari and A. Verma, A dual-ion imprinted polymer embedded in sol–gel matrix for the ultra trace simultaneous analysis of cadmium and copper, *Talanta*, 2014, **120**, 398–407.
6 T. Moreau, J. Lellouch, B. Juguet, B. Festy, G. Orssaud and J. R. Claude, Blood Cadmium Levels in a General Male Population with Special Reference to Smoking, *Arch. Environ. Health*, 1983, **38**, 163–167.
7 G. F. Nordberg, K. Nogawa and M. Nordberg, Chapter 32 - Cadmium in *Handbook on the Toxicology of Metals*, ed. G.F. Nordberg, B.A. Fowler, M. Nordberg, Academic Press, San Diego, 4th edn, 2015, pp. 667–716.
8 R. A. Bernhoft, Cadmium Toxicity and Treatment, *Sci. World J.*, 2013, **2013**, 394652.
9 M. Mezynska and M. M. Brzóska, *Environ. Sci. Pollut. Res.*, 2018, **25**, 3211–3232.
10 W. H. Organization, Evaluation of certain food additives and contaminants: thirty-third report of the joint FAO/WHO Expert Committee on food additives, in *Evaluation of certain food additives and contaminants: thirty-third report of the joint FAO/WHO expert committee on food additives*, 1989, p. 64.
11 C. Pettinari, A. Tăbăcaru and S. Galli, Coordination polymers and metal-organic frameworks based on poly(pyrazole)-containing ligands, *Coord. Chem. Rev.*, 2016, **307**, 1–31.
12 J. Klingele, S. Dechert and F. Meyer, Polynuclear transition metal complexes of metal···metal-bridging compartmental pyrazolate ligands, *Coord. Chem. Rev.*, 2009, **253**, 2698–2741.
13 X. Wang, X. Wang and Z. Guo, Metal-involved theranostics: An emerging strategy for fighting Alzheimer's disease, *Coord. Chem. Rev.*, 2018, **362**, 72–84.
14 A. P. Sadimenko and S. S. Basson, Organometallic complexes of heterocycles II. Complexes of pyrazoles, *Coord. Chem. Rev.*, 1996, **147**, 247–297.
15 J. Olguín and S. Brooker, Spin crossover active iron(II) complexes of selected pyrazole-pyridine/pyrazine ligands, *Coord. Chem. Rev.*, 2011, **255**, 203–240.
16 I. Castro, W. P. Barros, M. L. Calatayud, F. Lloret, N. Marino, G. De Munno, H. O. Stumpf, R. Ruiz-García and M. Julve, Dicopper(II) pyrazolenophanes: Ligand effects on their structures and magnetic properties, *Coord. Chem. Rev.*, 2016, **315**, 135–152.
17 E. V. Puttock, M. T. Walden and J. A. G. Williams, The luminescence properties of multinuclear platinum complexes, *Coord. Chem. Rev.*, 2018, **367**, 127–162.
18 J. Duan, W. Jin and S. Kitagawa, Water-resistant porous coordination polymers for gas separation, *Coord. Chem. Rev.*, 2017, **332**, 48–74.
19 K. X. Shang, S. Jing, D. C. Hu, X. Q. Yao, L. H. Zhi, C. D. Si and J. C. Liu, Six Ln (III) Coordination Polymers with a Semirigid Tetracarboxylic Acid Ligand: Bifunctional Luminescence Sensing, NIR-Luminescent Emission, and Magnetic Properties, *Cryst. Growth Des.*, 2018, **18**, 2112–2120.
20 S. I. Vasylevskyi, D. M. Bassani and K. M. Fromm, Anion-Induced Structural Diversity of Zn and Cd Coordination Polymers Based on Bis-9,10-(pyridine-4-yl)-anthracene, Their Luminescent Properties, and Highly Efficient Sensing of Nitro Derivatives and Herbicides, *Inorg. Chem.*, 2019, **58**, 5646–5653.
21 C. L. Liu, R. L. Zhang, C. S. Lin, L. P. Zhou, L. X. Cai, J. T. Kong, S. Q. Yang, K. L. Han and Q. F. Sun, Intraligand Charge Transfer Sensitization on Self-Assembled Europium Tetrahedral Cage Leads to Dual-Selective Luminescent Sensing toward Anion and Cation, *J. Am. Chem. Soc.*, 2017, **139**, 12474–12479.
22 Z. Dou, J. Yu, Y. Cui, Y. Yang, Z. Wang, D. Yang and G. Qian, Luminescent metal-organic framework films as highly sensitive and fast-response oxygen sensors, *J. Am. Chem. Soc.*, 2014, **136**, 5527–5530.
23 X. Zhang, X. Luo, N. Zhang, J. Wu and Y.-Q. Huang, A highly selective and sensitive Zn(ii) coordination polymer luminescent sensor for Al3+ and NACs in the aqueous phase, *Inorg. Chem. Front.*, 2017, **4**, 1888–1894.
24 S. Gama, I. Santos, F. Mendes, F. Marques, I. C. Santos, M. F. Carvalho, I. Correia, J. C. Pessoa and A. Paulo, Copper(II) complexes with tridentate pyrazole-based ligands: Synthesis, characterization, DNA cleavage activity and cytotoxicity, *J. Inorg. Biochem.*, 2011, **105**, 637–644.
25 I. F. Santos, G. P. Guedes, L. A. Mercante, A. M. R. Bernardino and M. G. F. Vaz, Synthesis, crystal structure and magnetism of three novel copper(II) complexes with pyrazole-based ligands, *J. Mol. Struct.*, 2012, **1011**, 99–104.
26 Y. Akhriff, J. Server-Carrió, A. Sancho, J. García-Lozano, E. Escrivá, J. V. Folgado and L. Soto, Synthesis, Crystal Structure, and Magnetic Properties of Oxalato−Copper(II) Complexes with 3,3-Bis(2-imidazolyl)propionic Acid, an Imidazole−Carboxylate Polyfunctional Ligand: From Mononuclear Entities to Ladder-Like Chains, *Inorg. Chem.*, 2002, **38**, 1174–1185.
27 B. H. Pearce, H. F. Ogutu and R. C. Luckay, Synthesis of Pyrazole-Based Pyridine Ligands and Their Use as Extractants for Nickel(II) and Copper(II): Crystal Structure

of a Copper(II)–Ligand Complex, *Eur. J. Inorg. Chem.*, 2017, 1189–1201.

28 S. Bhattacharyya, A. Sarkar, S. K. Dey, G. P. Jose, A. Mukherjee and T. K. Sengupta, Copper(ii) complex of methionine conjugated bis-pyrazole based ligand promotes dual pathway for DNA cleavage, *Dalton Trans.*, 2013, **42**, 11709–11719.

29 Y. Song, R. Fan, X. Du, K. Xing, Y. Dong, P. Wang and Y. Yang, Dual functional fluorescent sensor for selectively detecting acetone and Fe3+ based on {Cu2N4} substructure bridged Cu(i) coordination polymer, *RSC Adv.*, 2016, **6**, 110182–110189.

30 R. Kaur, A. Marwaha, V. A. Chhabra, K. Kaushal, K.-H. Kim and S. K. Tripathi, Facile synthesis of a Cu-based metal-organic framework from plastic waste and its application as a sensor for acetone, *J. Cleaner Prod.*, 2020, **263**, 121492.

31 G. A. van Albada, M. G. van der Horst, I. Mutikainen, U. Turpeinen and J. Reedijk, New 3,5-dimethylpyrazole copper(II) compounds with a variety of hydrogen bonds, synthesized by using a dehydrating agent: Synthesis, characterization, structures and intermolecular interactions, *Inorg. Chim. Acta*, 2008, **361**, 3380–3387.

32 X. Y. Chen, W. Z. Shen, P. Cheng, S. P. Yan, D. Z. Liao and Z. H. Jiang, Molecular and low-dimensional coordination compounds of copper(II) and 3,5-dimethylpyrazole - Synthesis, crystal structure, and properties, *Z. Anorg. Allg. Chem.*, 2003, **629**, 697–702.

33 F. Arjmand and M. Muddassir, Design and synthesis of heterobimetallic topoisomerase I and II inhibitor complexes: In vitro DNA binding, interaction with 5′-GMP and 5′-TMP and cleavage studies, *J. Photochem. Photobiol., B*, 2010, **101**, 37–46.

34 E. Szostak, A. Migdał-Mikuli and K. Orwat, Vibrational spectroscopy studies of solid–solid phase transitions in [Mg(OS(CH3)2)6](ClO4)2 and in its deuterated analogue, *Vib. Spectrosc.*, 2017, **89**, 123–130.

35 F. Arjmand, M. Muddassir and R. H. Khan, Chiral preference of l-tryptophan derived metal-based antitumor agent of late 3d-metal ions (Co(II), Cu(II) and Zn(II)) in comparison to d- and dl-tryptophan analogues: Their in vitro reactivity towards CT DNA, 5′-GMP and 5′-TMP, *Eur. J. Med. Chem.*, 2010, **45**, 3549–3557.

36 T. R. Cook, Y. R. Zheng and P. J. Stang, Metal-organic frameworks and self-assembled supramolecular coordination complexes: Comparing and contrasting the design, synthesis, and functionality of metal-organic materials, *Chem. Rev.*, 2013, **113**, 734–777.

37 B. Chen, Y. Yang, F. Zapata, G. Lin, G. Qian and E. B. Lobkovsky, Luminescent open metal sites within a metal-organic framework for sensing small molecules, *Adv. Mater.*, 2007, **19**, 1693–1696.

38 Z. Guo, H. Xu, S. Su, J. Cai, S. Dang, S. Xiang, G. Qian, H. Zhang, M. O'Keeffe and B. Chen, A robust near infrared luminescent ytterbium metal–organic framework for sensing of small molecules, *Chem. Commun.*, 2011, **47**, 5551–5553.

39 D. Ma, W. Wang, Y. Li, J. Li, C. Daiguebonne, G. Calvez and O. Guillou, In situ 2,5-pyrazinedicarboxylate and oxalate ligands synthesis leading to a microporous europium-organic framework capable of selective sensing of small molecules, *CrystEngComm*, 2010, **12**, 4372–4377.

40 F. Y. Yi, W. Yang and Z. M. Sun, Highly selective acetone fluorescent sensors based on microporous Cd(ii) metal-organic frameworks, *J. Mater. Chem.*, 2012, **22**, 23201–23209.

41 X. Zheng, L. Zhou, Y. Huang, C. Wang, J. Duan, L. Wen, Z. Tian and D. Li, A series of metal-organic frameworks based on 5-(4-pyridyl)-isophthalic acid: Selective sorption and fluorescence sensing, *J. Mater. Chem. A*, 2014, **2**, 12413–12422.

42 P. Zhang, C. Fu, Y. Xiao, Q. Zhang and C. Ding, Copper(II) complex as a turn on fluorescent sensing platform for acetylcholinesterase activity with high sensitivity, *Talanta*, 2020, **208**, 120406.

43 P. Kumar, R. Kaushik, A. Ghosh and A. D. Jose, Detection of moisture by fluorescent OFF-ON sensor in organic solvents and raw food products, *Anal. Chem.*, 2016, **88**, 11314–11318.

44 Y. Çimen, E. Ermiş, F. Dumludağ, A. R. Özkaya, B. Salih and Ö. Bekaroğlu, Synthesis, characterization, electrochemistry and VOC sensing properties of novel ball-type dinuclear metallophthalocyanines, *Sens. Actuators, B*, 2014, **202**, 1137–1147.

45 S. E.-d. H. Etaiw, H. Marie, E. M. Shalaby, R. S. Farag and F. A. Elsharqawy, Sensing and photocatalytic properties of nanosized Cu(I)CN organotin supramolecular coordination polymer based on pyrazine, *Appl. Organomet. Chem.*, 2019, **33**, e5114.

46 P. Ju, H. Yang, L. Jiang, M. Li, Y. Yu and E. Zhang, A novel high sensitive Cd-MOF fluorescent probe for acetone vapor in air and picric acid in water: Synthesis, structure and sensing properties, *Spectrochim. Acta, Part A*, 2021, **246**, 118962.

47 H. Pan, S. Wang, X. Dao and Y. Ni, Fluorescent Zn-PDC/Tb3+ Coordination Polymer Nanostructure: A Candidate for Highly Selective Detections of Cefixime Antibiotic and Acetone in Aqueous System, *Inorg. Chem.*, 2018, **57**, 1417–1425.

48 F.-Y. Yi, W. Yang and Z.-M. Sun, Highly selective acetone fluorescent sensors based on microporous Cd(ii) metal–organic frameworks, *J. Mater. Chem.*, 2012, **22**, 23201–23209.

49 J. D. Koch, J. Gronki and R. K. Hanson, Measurements of near-UV absorption spectra of acetone and 3-pentanone at high temperatures, *J. Quant. Spectrosc. Radiat. Transfer*, 2008, **109**, 2037–2044.

